Journal of Science and Technology, Vol. 43, No. 3 (2025), pp 1 - 22
© 2025 Kwame Nkrumah University of Science and Technology (KNUST)
https://dx.doi.org/10.4314/just.v43i3.1

IMPACT OF MINING ACTIVITIES ON LAND USE LAND COVER (LULC) USING GEOSPATIAL TECHNIQUES IN THE OBUASI MUNICIPALITY

Samira Naa Yemoley Nsiah[1], Jonathan Arthur Quaye-Ballard[1], Marfo Nimoh Jephthah[1]*, Titus Tienaah[1], Kwame Obeng[1], Tina Dzigbordi Wemegah[2], Precious Adwoa Okyere[3]

[1]Department of Geomatic Engineering, Kwame Nkrumah University of Science and Technology Kumasi, Ghana
[2]Accra Technical University, Accra, Ghana
[3]Department of Geography and Rural Development, Kwame Nkrumah University of Science and Technology, Kumasi, Ghana

***Corresponding author: quasimarfo@gmail.com**

ABSTRACT

Introduction: *Sustainable development, which balances economic, social, and environmental factors to meet the needs of the present and future generations, is a collective responsibility. Rapid population growth and intensification of socio-economic activities are causing significant changes in Land Use Land Cover (LULC), directly impacting ecosystem services, biodiversity, and climate. The Obuasi community is already facing environmental degradation and health problems due to gold mining.*

Methodology: *The study assessed the spatial extent and intensity of mining activities in the Obuasi Municipality on the LULC and predicted future LULC changes due to mining activities using geospatial techniques. The LULC changes were analysed using Landsat satellite imagery from 1990 to 2024 using a Random Forest (RF) classifier.*

Results and Discussion: *Mining Areas had a positive change of 27.655 km² (18.846%) while tailing dams and flooded pits increased by 46.655 km² (31.724%). Dense vegetation, less dense foliage, and built-up and bare land decreased by -34.692%, -8.024%, and -7.854%, respectively. These significant environmental changes show the need for effective land management strategies and geospatial techniques to monitor and mitigate adverse effects, promoting sustainable development policies and ecological resilience.*

Significance: *The findings of this study provide valuable insights into the environmental impacts of mining, emphasising the need to make informed research and policy decisions in the field of environmental science.*

Keywords: Land use land cover, Random Forest classifier, Geospatial techniques, Mining

INTRODUCTION

The Brundtland Commission defines sustainable development as the balance of economic, social, and environmental factors in decision-making that meets the needs of the present without compromising the ability of future generations to meet their own needs (Anarfi *et al.*, 2020; Brundtland, 1985). The concept of sustainable development emerged as a prominent development model and an integral part of popular international development discourse following the 1972 United Nations Conference on the Human Environment in Stockholm, which placed a strong emphasis on the importance of environmental protection (Anarfi *et al.*, 2020; Yiridomoh, 2021). LULC transformations directly impact ecosystem services, biodiversity, and climate because of the rapid population growth and the intensification of socio-economic activity (Awotwi *et al.*, 2018). Land degradation, together with local ecosystem devastation, is a result of disorderly land use activities, including shifting farming, uncontrolled urban expansion, and illegal mining. Also, agricultural land is lost to urbanisation and other forms of land use, including commercial, residential, and industrial activities. The process of urbanisation has resulted in significant alterations to Ghana's landscape and demographic composition (Cobbinah *et al.*, 2015). The rapid urbanisation of Ghana has exceeded the capacity for planning, placing pressure on the accessibility and availability of urban amenities such as housing and education (Toure *et al.*, 2020). The effects of land degradation present a significant challenge to the management of natural resources.

Since 1897, Obuasi, a town in Ghana with a significant mining industry, has been a major hub for gold mining (Antwi-Agyei *et al.*, 2009). The AngloGold Ashanti mine, which is among the ten largest in the world (Anglogold Ashanti, 2021), is a prominent example of the industry in the municipality. The gold mining industry in Obuasi has played a pivotal role in urbanisation and development, creating employment opportunities and infrastructure for the local population. Ghana's rich natural resources and strong mining industry, which have expanded significantly in recent years, are key pillars of the economy (Opoku *et al.*, 2015). Despite these encouraging signs, the overall contribution of the mining industry to Ghana's economic development is challenged by the negative impacts experienced by mining communities. Gold mining also gives rise to environmental concerns, including pollution, deforestation, the loss of biodiversity, human displacement, the disruption of livelihoods, and migration (Anarfi *et al.*, 2020). Mining activity has resulted in cropland and forest areas being degraded to bare and unproductive regions (Awotwi *et al.*, 2018) due to a combination of unpredictable income and climate challenges (Nyame & Blocher, 2010). This may have the effect of undermining the livelihoods of some locals, particularly farmers, in these areas as they shift towards small-scale mining activities (Basommi *et al.*, 2016; Nyame & Blocher, 2010).

As migrant workers flood into mining communities in search of better livelihoods, housing units become prohibitively expensive. This situation creates social inequality, with property owners exploiting the demand for housing to the detriment of the local population. The Obuasi community faces challenges due to the loss of arable land due to mining operations, which threatens income sources, limits coping strategies, and perpetuates poverty (Pereira *et al.*, 2021). Additionally, the susceptibility of one's livelihood to environmental changes creates a division between those who benefit from mining and those who are impoverished by it, leading to conflicts within communities (Ros-Tonen *et al.*, 2021). Educational attainment significantly impacts employability and economic status in the mining economy, leading to feelings of exclusion and embitterment for those lacking education (Adu-Baffour *et al.*, 2021). The influx of migrants into mining areas, such as Obuasi, has also led to increased social vices, including higher incidences of criminal activities and promiscuous lifestyles (Ababio & Mensah, 2011).

Mahoney *et al.* (2015) support the widely accepted notion that intensive and prolonged mining activities in a region lead to negative impacts on the environment. (Aram *et al.*, 2021) emphasise that the severity of these impacts depends on factors such as the technology used, the scale of the extraction operation, and the location of the project. The environmental impacts of mining are closely linked to its health consequences. Malaria outbreaks are often due to mosquitoes breeding in stagnant water bodies and tailings dams contaminated by mining activities. Respiratory diseases are primarily caused by air pollution resulting from open pits and processing plants, which release dust and other harmful particulates into the atmosphere (Gbedzi *et al.*, 2022; Yeboah, 2008). Skin infections, fever, and diarrhoea are frequently reported among residents who consume water from polluted rivers and other contaminated water sources (Aram *et al.*, 2021). In Obuasi, statistical data reveal a high prevalence of Upper Respiratory Tract Infections (URTI), malaria, and skin diseases among the local population (Kwaning & Atteh, 2022). Mining activities in the Tarkwa area have been associated with a range of health issues, both physical and mental (Yeboah, 2008). The toxic environment created by mining operations and the high-stress nature of the work contribute significantly to these health problems (Kwaning & Atteh, 2022). Mining is widely regarded as one of the most hazardous occupations globally (Pereira *et al.*, 2021). Moreover, the use of toxic chemicals like cyanide and mercury in mining processes poses severe health risks to workers. Exposure to these chemicals can lead to heat exhaustion, elevated blood pressure, nervous system disorders, and myocardial infarction (Basu *et al.*, 2015). Cyanide, used in the gold extraction process, is highly toxic and can cause acute poisoning, resulting in respiratory failure or even death if proper safety measures are not in place. Mercury, often used in small-scale mining operations, can cause severe neurological damage, impacting cognitive functions and motor skills. Chronic exposure to these chemicals not only affects the workers but can also contaminate local water supplies, further endangering community health. According to Kwaning & Atteh (2022), Action Aid reported in 2006 that the large amount of water used in mining, along with the installation of tailing dams to manage ore extraction residues, leads to the presence of persistent poisons such as arsenic and cyanide (Ros-Tonen *et al.*, 2021). These pollutants significantly degrade water quality, making it unsafe for all forms of life and posing a threat to the survival and economic well-being of local communities (Faseyi *et al.*, 2022; Ros-Tonen *et al.*, 2021). Surface and underground mining operations that use explosives also cause noise and vibrations, further contributing to pollution in these areas (Kwaning & Atteh, 2022).

With technology, community engagement, enforcement, and regulation, the Government of Ghana has put in place a comprehensive plan to combat illegal mining. The government has updated the Mining Act to include stricter penalties both for obtaining a mining license and for engaging in illegal mining. The Minerals and Mining Act, 2006 (Act 703)[1] was amended to increase penalties for illegal miners and those who assist in illegal operations. The government introduced the Community Mining Scheme in 2017, which

---

[1] https://mlnr.gov.gh/wp-content/uploads/2019/06/Minerals-Mining-Amendment-Act-2015-ACT-900-1

allows for small-scale, regulated mining in local communities, along with Operation Vanguard[2], a joint military-police task force. The use of drones to monitor mining activities and digital tracking systems for the movement and transport of equipment are examples of technological interventions. Also, public awareness campaigns and engagement with traditional authorities are being conducted to educate the populace about the environmental and social impacts of illegal mining. Despite all these measures, there have been increasing mining activities and licensing issuance recently. According to the Ghana Mining repository[3], between 1988 and 2025, about 2,250 mining and mining-related licenses have been issued. Between 1988 and 2008, a total of 40 mining permits were issued. Subsequently, from 2009 to 2016, this number rose to 59 permits. Furthermore, from 2017 to 2024, an impressive 2,151 mining licenses were[4] issued. Therefore, a cost-effective land use monitoring technique is required for better planning, management, and sustainable development of available natural resources for present and future generations.

The availability of Remote Sensing (RS) data enables the assessment and monitoring of changes in land use and land cover (Cheruto *et al.*, 2016). The continued development and improvement of RS technology have led to the creation of more sophisticated instruments capable of detecting changes on the surface. These improvements have been made in terms of temporal and geographical resolution, as well as spectral resolution, allowing for more detailed analysis. The analysis of remotely sensed data has been widely employed to evaluate the effects of various anthropogenic activities on ecosystems such as mining (Awotwi *et al.*, 2018; Basommi *et al.*, 2015; Ngom *et al.*, 2023; Sarma & Kushwaha, 2005), agriculture (Adão *et al.*, 2017; Gandharum *et al.*, 2022), deforestation (Amankwah *et al.*, 2021; Brovelli *et al.*, 2020; Koranteng & Zawila-Niedzwiecki, 2015; Yordanov & Brovelli, 2021), urbanisation (Ashiagbor *et al.*, 2019; Gondwe *et al.*, 2021; Mahboob *et al.*, 2015; Singh *et al.*, 2017), water quality (Gbedzi *et al.*, 2022; Marfo *et al.*, 2024), and land degradation (El Baroudy, 2011; Mohamed *et al.*, 2013).

While recent work highlights the role of remote sensing in environmental monitoring (Amoako-Attah, 2024), few studies have attempted to assess the direct impacts of mining activities upon LULC changes in Obuasi using geospatial techniques. In addition, the predictive modelling of LULC changes induced by mining activities remains underexplored, making it difficult to anticipate future environmental impacts. The study assessed the spatial extent and intensity of mining activities on Land Use Land Cover (LULC) changes in the Obuasi Municipality using geospatial techniques. Also, the study assessed and predicted the environmental impacts of mining on LULC. This study will guide sustainable land management and policymaking in Obuasi, providing a comprehensive understanding of how mining activities have changed and continue to affect land use and land cover, facilitating informed decision-making for sustainable development.

MATERIALS AND METHODS

Study Area

The Obuasi Municipality is in the Ashanti Region of Ghana, 64 km south of Kumasi. It lies between latitudes 6° 6′ 0″ and 6° 20′ 0″ N and longitudes 1° 36′ 0″ and 1° 50′ 0″ W (Figure

---

[2] operationvanguard.mil.gh
[3] https://ghana.revenuedev.org/license
[4] https://www.myjoyonline.com/over-2000-mining-and-related-licenses-issued-since-2017/

1). Obuasi, which is also the administrative centre of the region, is home to the well-known and thriving Anglo Gold Ashanti (formerly known as Obuasi Gold Mine). The Obuasi Municipality has a semi-arid climate with two distinct maximum rainfall regimes. The average annual rainfall is between 1250 and 1750 mm. March is the hottest month of the year, with an average maximum temperature of 30°C. There is a constant high temperature throughout the year. However, the average annual temperature is 25.5°C. Relative humidity is high (75% to 80%) during the rainy season (Ghana Regions, 2022). The primary vegetation type is degraded semi-deciduous forest. There are a few hardwood species in the forest that are harvested for timber. Within its concession, AngloGold Ashanti has maintained large areas of teak plantations as green belts. According to the 2021 Population and Housing Census, the municipality has a population of 104,297 (Ghana Statistical Service, 2021). The area has a predominantly agricultural workforce despite its abundant natural resources. The local economy is heavily dependent on mining and related industries.

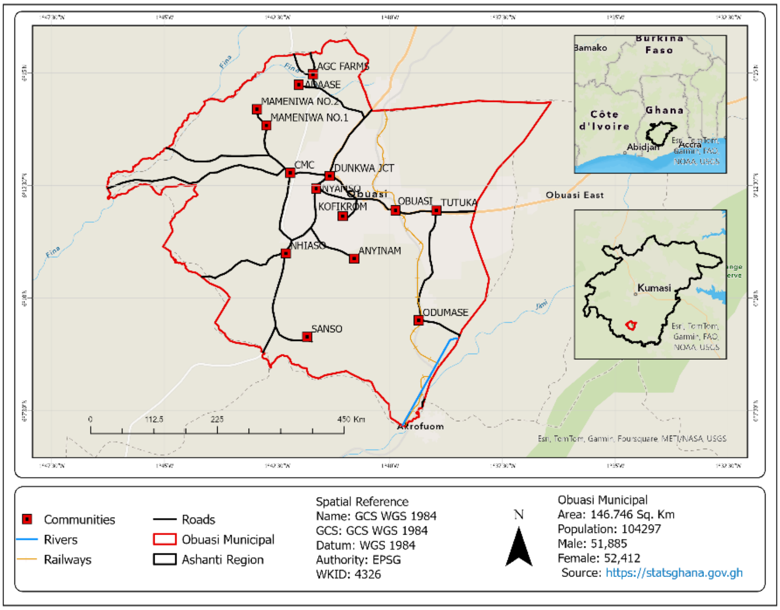

Figure 1: Map of Obuasi Municipal

Satellite Data Sources and Collection

The images for the study were Landsat (5, 7, and 8) and digital elevation model (DEM) images retrieved from the Google Earth Engine (GEE) dataset catalogue for the years 1990, 2008, 2016, and 2024 which cover the entire Obuasi metropolis. The Landsat 5 satellite has a Thematic Mapper (TM) and a Multispectral Scanner (MSS). The TM has 6 spectral bands with a spatial resolution of 30 meters and one thermal band having a spatial resolution of 120 meters while the MSS had 4 spectral bands with a spatial resolution of 80 meters (Loveland & Dwyer, 2012; Zareie *et al.*, 2016). Also, the Landsat 7 uses the Enhanced Thematic Mapper Plus (ETM+) sensor for its operations. The sensor has a panchromatic band (15m resolution), a thermal band (60m resolution) and 8 spectral bands

(30m resolution) (Loveland & Dwyer, 2012). However, Landsat 8 has the Operational Land Imager Sensor (OLIS) instrument, and the Thermal Infrared Sensor (TIRS) onboard the satellite, which can now deliver pixel values across a 12-bit range, encompassing 4,096 levels. The OLIS has 8 spectral bands (30m resolution) and a panchromatic band (15m resolution) while the TIRS has 2 thermal bands with a 100m resolution (Loveland & Irons, 2016). Subsequently, in this study, only satellite images with a minimum of 10 % cloud cover were acquired and used for the LULC classification to reduce errors that may result from cloud cover interference during analysis.

Image Classification and Accuracy Assessment

Google Earth Pro was used to select the training samples and validation points. Different classes, including less dense vegetation, dense vegetation, tailings dams, flooded pits, built-up and bare land, and mining areas, were given unique names. Samples were selected using Google Earth Pro by visually assessing satellite imagery and marking areas of interest. 70% (700 training points) of the samples were used for training, while 30% (300 training points) were used for validation. Google Earth Engine (GEE) was used for categorisation and accuracy assessment, followed by visual interpretation using Google Earth Pro for all further sampling. Primary land cover conversion from 1990 to 2024 was mapped to determine the geographical pattern and process and to assess the impact of LULC changes on the Obuasi Municipality. The classification was made according to the relevant previous studies and the LULC currently present in the study area. The methodological process is illustrated in Figure 2.

The Land cover categories were effectively mapped using RF classifiers (supervised classification) on Landsat imagery, digital elevation model, and vegetation indices in the Google Earth Engine (GEE). It is the most adaptable and user-friendly machine learning model for land classification (Zhou *et al.*, 2020). RF models use randomly selected data samples to make decisions (Pachón *et al.*, 2018). This is based on predictions made by each ‘tree’, with the best decision being chosen by popular vote. The RF classification approach, which is crucial for determining the importance of each variable, was used to quantify the contribution of each class to the classification result (Matarira *et al.*, 2022). Five decision trees were selected for the study to increase classification accuracy while reducing overfitting. However, to improve feature differentiation, the input features consisted of a DEM and spectral bands from Landsat imagery. More precisely, Landsat 5, Landsat 7, and Landsat 8/9 used six spectral bands and a DEM, seven spectral bands and a DEM, and six spectral bands and a DEM, respectively.

In this study, different forms of land cover were used, based on Anderson’s Level I Classification Scheme (Anderson, 2007), and divided into five categories: Less dense vegetation, dense vegetation, tailings dams and flooded pits, built-up and bare land, and mining areas. Land cover and land use are classified into four primary groups according to Anderson’s Level I Classification Scheme: water, agriculture and grazing, urban and industrial, and conservation and recreation. Dense vegetation is subdivided into three types, with less dense vegetation classified as cropped and grazed. Human settlements are included in urban and industrial regions, while water includes all bodies of water. Areas that are not listed are not considered to be classified. The LULC classification scheme used in this study is shown in Table 1.

Table 1: LULC Categorization Scheme (adopted from (Anderson, 2007))

LULC Classes	Description of Land Use Land Cover Classes
Less dense vegetation	Areas covered with grasses, croplands, areas with a vegetative cover of less than 10%, and Shrubs.
Dense vegetation	Areas with tree canopy above 10%,
Tailing dams and flooded pits	Streams and open galamsey pits, flooded areas, Lakes, Ponds, Reservoirs, and swimming pools.
Built-ups and bare land	Includes physical structures such as residential, commercial, industrial, roads, bare lands, etc.
Mining Area	Bare Lands due to the lack of vegetation cover and the presence of exposed land resulting from mining activities by large-scale corporate miners (AngloGold Ashanti) and artisanal miners corporate mining and artisanal miners..

The area for each land cover class was calculated from the pixel counts for each distinct class, and the corresponding percentages were determined. These values were then used to calculate the rate of change, the annual rate of change, and their respective percentages. The results were visually presented in graphs illustrating the rate of change. Equations 1 and 2 were used to calculate the annual rate of change and the percentage rate of change.

$$Annual\ Rate\ (A) = \frac{Areax\ {+1}{-}Area\ x}{Tyears} \quad \textbf{eqn 1}$$

$$Percentage\ Rate = \frac{Annual\ rate\ of\ change}{\sum_{k=1}^{n} Areax{*}Tyears} * 100 \quad \textbf{eqn 2}$$

where Area$_{x\,=}$ Area of each class, Area$_{x+1}$= Area of the corresponding class in the preceding year, T$_{years}$ = Difference in years, $\sum_{k=1}^{n}$ = Total area corresponding to each year.

The last stage of the supervised classification process represents the final output stage. The final output of the classification process may either be produced as a thematic or classification map, with each map representing each class of interest. LULC classification relies on assessing the accuracy of classified data or output maps. Results may not accurately represent original data and may contain errors. Analysts must characterise these errors before use. Ground truthing, a widely recognised approach, involves collecting training data from sample sites through field reconnaissance. This comparison uses an error matrix to quantify the accuracy of each categorised map, as well as the total map accuracy (Overall Accuracy), which combines all classes. Accuracy assessment signifies the reliability and replication of the thematic classification generated by the analyst's methods. In land-use/cover-related projects, an error matrix is generated to assess class accuracies based on the category of classes classified (Nelson *et al.*, 2020). Accuracy was assessed quantitatively by calculating the overall accuracy (the ratio of correctly classified pixels to the total number of sampled pixels) and the kappa coefficient. The interpretation of the kappa values is as follows: a kappa value of less than 0 indicates no agreement; 0-0.2 indicates slight agreement; 0.2-0.41 indicates fair agreement; 0.41-0.6 indicates moderate agreement; 0.6-0.8 indicates substantial agreement, and 0.81-1.0 indicates almost perfect agreement. A kappa value of 1 indicates perfect agreement, whereas a kappa value of 0 indicates no agreement. The kappa coefficient was determined using equation 3.

$$\mathrm{k} = \frac{N\sum_{i=1}^{n} mi,i - \sum_{i=1}^{n}(GiCi)}{N^2 - \sum_{i=1}^{n}(GiCi)} \quad \textbf{eqn 3}$$

where i = the class number; n = the total number of classified pixels compared to the reference pixels; mi, i = the number of values belonging to the reference class i that have also been classified as class I (pixels found in both the reference and classified maps); Ci = the total number of predicted pixels belonging to class i; and Gi = the total number of reference pixels belonging to class i.

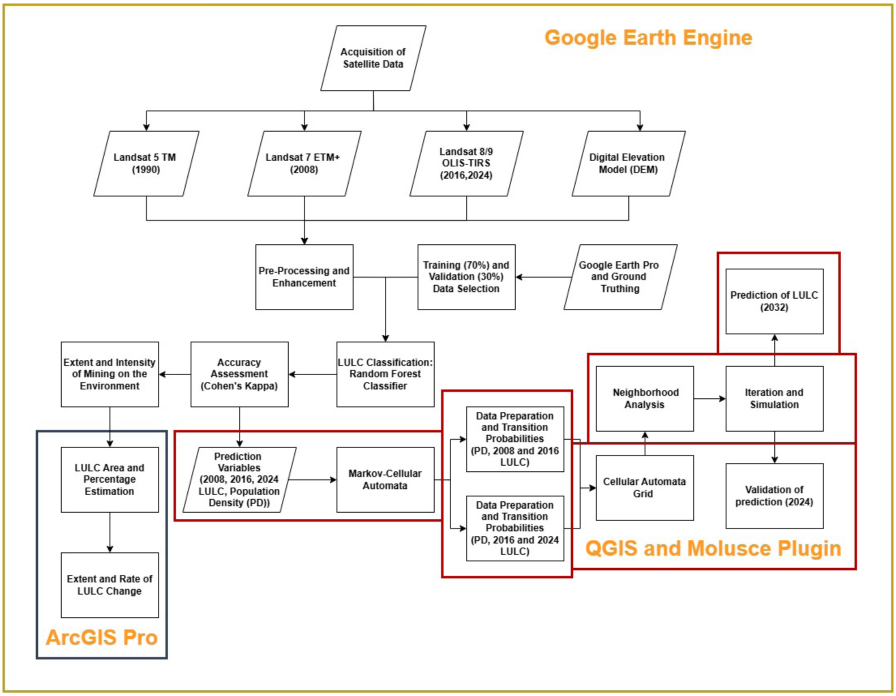

Figure 2: Methodological Flowchart

RESULTS

LULC Classification from 1990 to 2024

In 1990, dense vegetation occupied a total area of 77.830 km^2, less dense vegetation covered an area of 35.855 km^2, and settlement and bare land also covered 33.061 km^2. Their respective percentages were 53.037%, 24.433%, and 22.529%. In 2008, dense vegetation occupied a total area of 68.493 km^2, less dense vegetation covered an area of 37.566 km^2, settlement, and bare land also covered 15.045 km^2, and Mining Areas covered 21.402 km^2 while tailing dams and flooded areas covered 4.240 km^2. In 2016, dense vegetation occupied a total area of 53.972 km^2, representing 36.779%. Less dense vegetation covered an area of 42.037 km^2, covering 28.646% of the land total area, and settlement and bare land also covered 20.452 km^2 (13.937%). Mining Areas covered 17.015 km^2 (11.595%) while tailing dams and flooded areas covered 13.270 km^2, representing 9.043% of the total land area. In 2024, dense vegetation occupied a total area of 26.921 km^2, representing 18.346%; less dense vegetation covered an area of 24.081 km^2, covering 16.410% of the land's total area. Settlement and bare land also covered 21.535 km^2 (14.675%), and Mining Areas covered 27.655 km^2 (18.846%) while tailing dams and flooded areas covered 46.554 km^2, representing 31.724 % of the total land area. Figure 3 shows the LULC distribution map for 1990, 2008, 2016, and 2024. Table 2 shows the area in square kilometres covered by the various land-use types and changes for the years 1990, 2008, 2016, and 2024. Figure 4 is a bar chart showing the distribution of the land use land cover classes from 1990 to 2024. Table 3 shows the kappa results and overall statistics, defining the accuracy of the classified maps of the various Land-use types in the Obuasi Municipal.

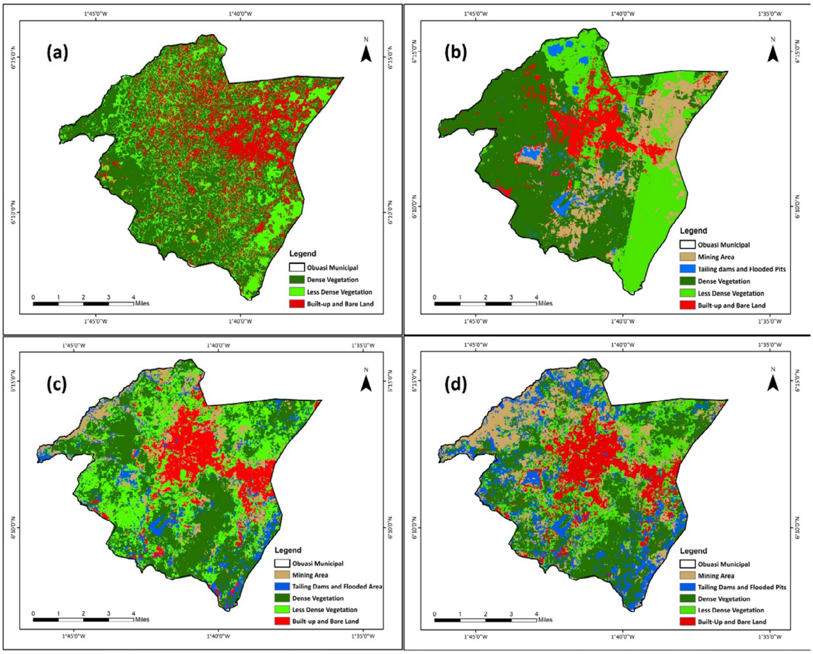

Figure 3: LULC distribution map of Obuasi municipal (a) 1990; (b) 2008; (c) 2016; (d) 2024

Table 2: Land-use land cover class area statistics in km^2 from 1990 to 2024

Year	Area (km sq)/Percentage (%)	MA	TD-FA	DV	LDV	BU-BL
1990	Area (km sq)	0.000	0.000	77.830	35.855	33.061
	Percentage (%)	0.000	0.000	53.037	24.433	22.529
2008	Area (km sq)	21.402	4.240	68.493	37.566	15.045
	Percentage (%)	14.585	2.889	46.675	25.599	10.252
2016	Area (km sq)	17.015	13.270	53.972	42.037	20.452
	Percentage (%)	11.595	9.043	36.779	28.646	13.937

2024	Area (km sq)	27.655	46.554	26.921	24.081	21.535
	Percentage (%)	18.846	31.724	18.346	16.410	14.675
1990-2008	Area (km sq)	21.402	4.240	-9.337	1.711	-18.016
	Percentage (%)	14.585	2.889	-6.363	1.166	-12.277
2008-2016	Area (km sq)	-4.387	9.030	-14.522	4.471	5.407
	Percentage (%)	-2.990	6.154	-9.896	3.047	3.685
2016-2024	Area (km sq)	10.640	33.283	-27.050	-17.957	1.083
	Percentage (%)	7.251	22.681	-18.433	-12.236	0.738
1990-2024	Area (km sq)	27.655	46.554	-50.909	-11.775	-11.526
	Percentage (%)	18.846	31.724	-34.692	-8.024	-7.854

MA= mining areas; TD-FA= tailing dams and flooded areas; DV= dense vegetation; LDV= less dense vegetation; BU-BL= built-up and bare land.

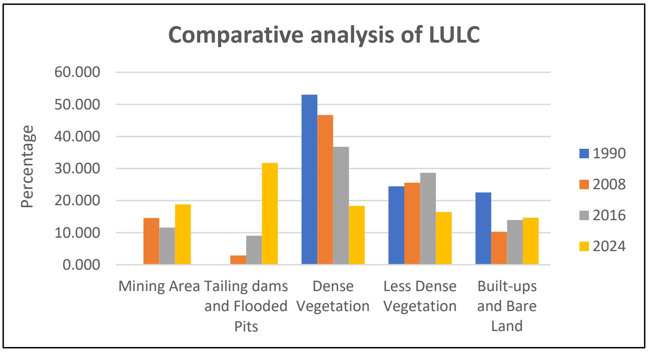

Figure 4: Distribution of LULC from 1990 to 2024

Table 3: Accuracy Assessment of the LULC classified images from 1990 to 2024

YEAR	**1990**		**2008**		**2016**		**2024**	
LULC	**PA**	**UA**	**PA**	**UA**	**PA**	**UA**	**PA**	**UA**
MA	0.000	0.000	0.941	0.842	0.954	0.873	0.972	0.930
TD-FA	0.000	0.000	0.925	0.974	0.929	0.939	0.913	0.950
DV	1.000	1.000	0.964	0.794	0.918	0.935	0.970	0.914
LDV	1.000	0.667	0.816	0.912	0.906	0.941	0.855	0.922
BU-BL	0.750	1.000	0.872	0.971	0.936	0.962	0.960	0.951
Overall Accuracy	0.859		0.899		0.911		0.933	
Kappa	0.909		0.874		0.929		0.916	

MA = mining areas; TD-FA = tailing dams and flooded areas; DV = dense vegetation; LDV = less dense vegetation; BU-BL= built-up and bare land; PA = Producer Accuracy; UA= User Accuracy

LULC change from 1990 to 2024

From 1990 to 2024, dense vegetation had a negative change of 50.909 km^2, representing 34.692%. Less dense vegetation had a negative change of 11.775 km^2, which represents 8.024%, and built-up and bare land had a negative change of 11.526 km^2, which represents 7.854%. Mining Areas also had a positive change of 27.655 km^2, representing 18.846%, while tailing dams and flooded pits had an overall positive change of 46.655 km^2, which represents 31.724%. Table 2 shows the area of change in km^2 covered by the various land-use types from 1990 to 2024. Figure 5 shows the distribution of LULC changes from 1990 to 2024.

Figure 5: Distribution of the rate of change of the LULC classes from (a) 1990-2024, (b) 1990-2008, (c) 2008-2016, and (d) 2016-2024

Dense vegetation areas (Figure 6a) saw a decrease of 9.337 km^2, or 6.363%, from 1990 to 2008. This decline continued from 2008 to 2016, with a further reduction of 14.522 km^2, representing a 9.896% decrease. The trend persisted from 2016 to 2024, with dense vegetation decreasing by 27.050 km^2, a substantial decline of 18.433%. Less dense vegetation (Figure 6b) increased by 1.711 km^2, or 1.166%, from 1990 to 2008. From 2008 to 2016, there was a further increase of 4.471 km^2, representing a 3.047% rise.

However, this trend reversed from 2016 to 2024, with less dense vegetation decreasing by 17.957 km^2, a 12.236% decline. From 1990 to 2008, mining areas (Figure 6c) increased by 21.402 km^2, representing a 14.585% rise. However, between 2008 and 2016, mining areas decreased by 4.387 km^2, a 2.990% decline. The trend reversed again from 2016 to 2024, with mining areas growing by 10.640 km^2, a 7.251% increase.

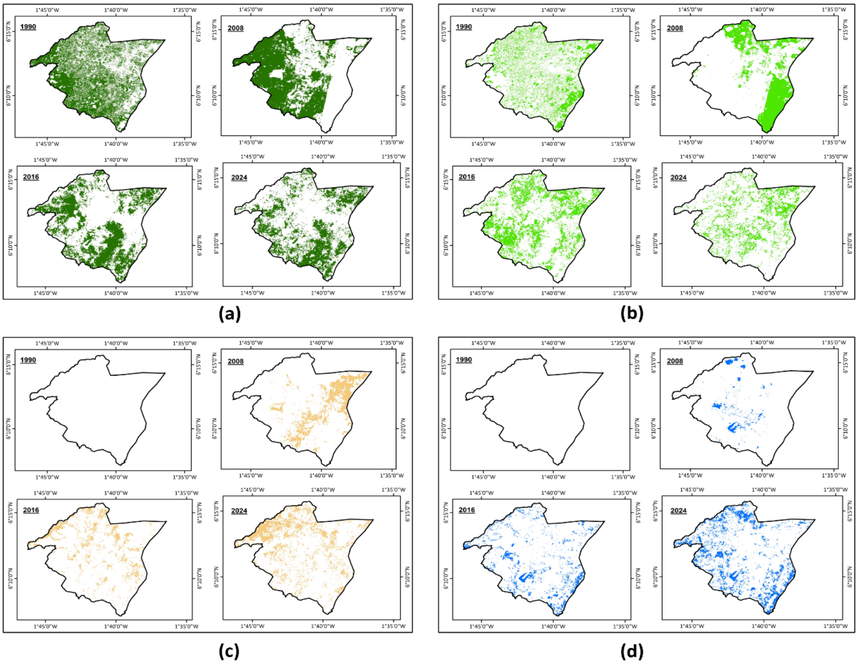

(a) (b)

(c) (d)

Figure 6: Change map for (a) Dense vegetation; (b) Less dense vegetation; (c) Mining areas; and (d) Tailing dams and flooded pits from 1990 to 2024

Between 1990 and 2008, tailing dams and flooded areas (Figure 6d) increased by 4.240 km², a 2.889% rise. This trend continued from 2008 to 2016, with an increase of 9.030 km², or 6.154%. From 2016 to 2024, there was a dramatic rise of 33.283 km², representing a 22.681% increase. Overall, from 1990 to 2024, these areas grew by 46.554 km². Built-up and bare land (Figure 7a) decreased by 18.016 km², or 12.277%, from 1990 to 2008. From 2008 to 2016, these areas increased by 5.407 km², representing a 3.685% rise. The trend continued with a modest increase of 1.083 km², or 0.738%, from 2016 to 2024. Overall, from 1990 to 2024, built-up and bare land decreased by 11.526 km².

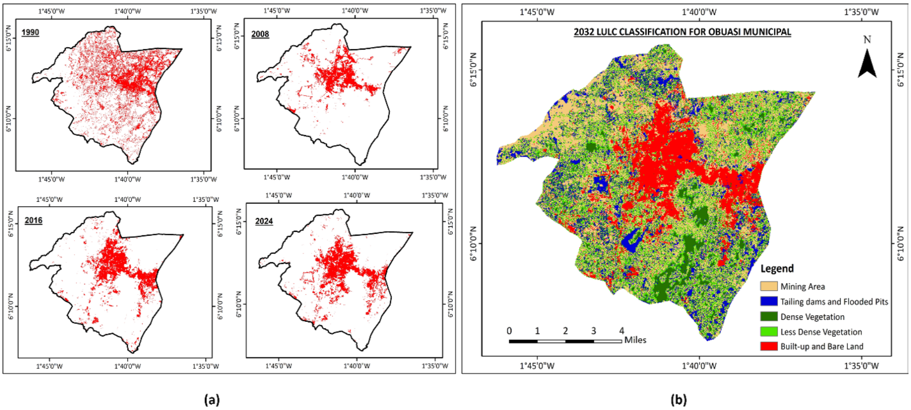

(a) (b)

Figure 7: (a) Change map for Built-ups and Bare Land from 1990-2024; (b) 2032 predicted LULC Map

Redicting future LULC Changes due to Mining Activities

In 2032 (Figure 7b), dense vegetation occupied a total area of 18.179 km^2, representing 12.388%. Less dense vegetation covered an area of 31.717 km^2, covering 21.613% of the land's total area, and built-ups and bare land also covered 25.529 km^2 (17.397%). Mining Areas covered 52.179 km^2 (35.558%) while tailing dams and flooded areas covered 19.141 km^2, representing 13.044% of the total land area. Table 4 shows the area of change in km^2 covered by the various land-use types between 2024 and 2032. Figure 8a shows the LULC distribution from 2024 to 2032. Figure 8b shows the distribution of LULC changes from 2024 to 2032.

Table 4: LULC change from 2024 to 2032

Year	Area (km sq)/Percentage (%)	MA	TD-FA	DV	LDV	BU-BL
2024	Area (km sq)	27.655	46.554	26.921	24.081	21.535
	Percentage (%)	18.846	31.724	18.346	16.410	14.675
2032	Area (km sq)	52.179	19.141	18.179	31.717	25.529
	Percentage (%)	35.558	13.044	12.388	21.613	17.397
2024-2032	Area (km sq)	24.524	-27.412	-8.742	7.636	3.994
	Percentage (%)	16.712	-18.680	-5.957	5.204	2.722

MA = mining areas; TD-FA = tailing dams and flooded areas; DV = dense vegetation; LDV = less dense vegetation; BU-BL = built-up and bare land.

From 2024 to 2032, dense vegetation experienced a negative change of 8.742 km^2, representing 5.957%. Less dense vegetation had a positive change of 7.636 km^{2,} which represents 5.204%, and built-up and bare land had a positive change of 3.994 km^{2,} which represents 2.722 %, and Mining Areas also had a positive change of 24.524 km^{2,} representing 16.712%. In comparison, tailing dams and flooded pits had an overall negative change of 27.412 km^2, which is 18.680%.

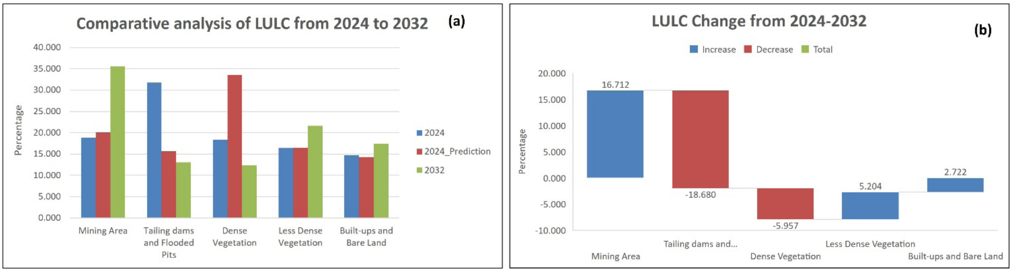

Figure 8: (a) Distribution of LULC from 2024 to 2032; and (b) Distribution of rate of change of the LULC classes from 2024 to 2032

LULC data from 2008 and 2016 served as the basis for the model's identification of transition patterns and its projection of LULC changes in the future. The model assumed and used land cover transition patterns observed between 2016 and 2024, and population density to predict the future changes. To test the validity and reliability of the model, it was first used to predict LULC in 2024 using the 2008 and 2016 datasets. The validation of the predicted 2024 LULC was assessed using the 2024 LULC map. Based on the predictions and validation of the LULC classification for 2024 using the QGIS 2.8 Mollusce plugin, the results indicate high accuracy levels. Additionally, the prediction model assumes that key driving factors, such as mining expansion, urbanisation, and vegetation trends, follow their past patterns. The overall percentage correctness of the classification is 84.052%, with various Kappa statistics suggesting substantial agreement between the predicted and actual classifications. Specifically, the overall Kappa is 0.838, the histogram Kappa is 0.868, and the locational Kappa is 0.798.

DISCUSSION

Evaluating the spatial extent and intensity of mining activities in Obuasi Municipality

A comprehensive overview of the changes in LULC in the Obuasi Municipality over 32 years, from 1990 to 2022, is provided by the data in Table 2 and Figure 4. Mining areas, tailings dams, and flooded areas, dense vegetation, less dense vegetation, built-up and bare land are the primary land use classes analysed in this study. Mining areas increased significantly from 0 km² in 1990 to 27.655 km² in 2024, representing 18.846% of the total land area. Similarly, tailings dams and flooded pits show a significant increase from 0 km² in 1990 to 46.554 km² in 2024, representing 31.724% of the total land area. In contrast, the area of dense vegetation will decrease significantly from 77.830 km² (53.037%) in 1990 to 26.921 km² (18.346%) in 2024. The area of less dense vegetation will also decrease from 35.855 km² (24.433%) in 1990 to 24.081 km² (16.410%) in 2024. Built-up and bare land decreased from 33.061 km² (22.529%) in 1990 to 15.045 km² (10.252%) in 2008 but increased to 21.535 km² (14.675%) in 2024. According to the Ellimah (2022), the reopening of the Obuasi mine in 2019 has contributed to economic growth that has increased employment opportunities, business revitalisation and population growth. The community's built-up areas have therefore grown because of this economic recovery.

From 1990 to 2008, as shown in Figure 5b, there was a significant increase in mining areas of 21.402 km² (14.585%) and in tailings dams and flooded areas of 4.240 km² (2.889%). The tailings dams were created because of the mining pits that the miners left behind after they had extracted the gold. These pits are then filled with rainwater and with the water that is used in the drilling and mining process (Kossoff *et al.*, 2014). However, during this period, there was also a decrease in dense vegetation of 9.337 km² (-6.363%) and a decrease in built-up and bare land of 18.016 km² (-12.277%). Adu-Poku *et al.* (2012) also reported a similar trend in forest loss and reduction in barren lands within the Obuasi municipality between 1986 and 2008.

Subsequently, from 2008 to 2016 (Figure 5c), mining areas decreased slightly by 4.387 km² (-2.990%), while tailings dams and flooded areas increased significantly by 9.030 km² (6.154%). The decline in mining activity was a result of the temporary closure of AngloGold Mining in 2014. However, illegal miners - miners who lost their jobs after AngloGold Ashanti halted operations and those who lost their jobs before AngloGold Ashanti halted operations - emerged in Obuasi to invade AngloGold Ashanti's mineral concessions as asserted by Opoku; *et al.* (2015) and Yankson & Gough (2019). These miners used traditional tools like pickaxes and shovels to dig pits in search of minerals and leave the pits filled with water used for washing the mineral ore and rainwater. AngloGold Ashanti had to fight these illegal miners using government law enforcement agencies and private security guards (Yankson & Gough, 2019). These actions contributed to the reduction of mining areas in the Obuasi community and increased the area for tailings dams, and flooded pits. Between 2016 and 2024 (Figure 5d), mining activity intensified with an increase of 10.640 km² (7.251%) in mined areas and 33.283 km² (22.681%) in tailings dams and flooded areas. This increase in mining activity led to a significant decrease in dense vegetation of 27.050 km² (-18.433%) and less dense vegetation of 17.957 km² (-12.236%). Awotwi *et al.* (2018) conducted research in the Pra River Basin, where mining led to comparable LULC changes. They found that galamsey activities result in a reduction of forests and less dense vegetation due to unreclaimed mined land rendered infertile by chemicals used in mineral extraction. Farmers are forced to destroy these forests and other less dense vegetation to continue farming. During this period, extensive deforestation and landscape alteration underlined the peak impact of mining activities on land cover.

Over the entire period from 1990 to 2024 (Figure 5a), the trend is towards the expansion of mining operations, with an increase of 27.655 km² (18.846%) in mining areas and 46.554 km² (31.724%) in tailings dams and flooded areas. In addition, there was a notable overall decrease in dense vegetation of 50.909 km² (-34.692%), as well as decreases in less dense vegetation and built-up and bare land of 11.775 km² (-8.024%) and 11.526 km² (-7.854%) respectively. These extensive changes reflect the long-term and widespread environmental impact of mining activities over decades.

Assessing the Environmental Impacts of Mining on LULC

Between 1990 and 2008, there was a significant increase in mining areas of 21.402 km² (14.585%) and in tailings dams and flooded areas of 4.240 km² (2.889%). This expansion reduced dense vegetation by 9.337 km² (-6.363 %) and built-up and bare land by 18.016 km² (-12.277%). A similar reduction of forest areas was observed by Mensah *et al.* (2017) in the Prestea-Huni Valley district as a result of mining activities between the years 2002 and 2008. The decrease in dense vegetation is indicative of significant deforestation and habitat loss. At the same time, the increase in tailings dams and flooded pits is indicative of water pollution as the chemicals these miners use during the extraction processes are poisonous and have health implications on humans and animals asserted by Kwaning & Atteh (2022), Mensah *et al.* (2015), and Nunoo *et al.* (2022). Also, the gases and noise during the extraction processes cause environmental pollution.

From 2008 to 2016, mining areas decreased by 4.387 km² (-2.990%), but tailings dams and flooded areas increased significantly by 9.030 km² (6.154%). In addition, the area of dense vegetation continued to decrease by 14.522 km² (-9.896%), indicating continued depletion of the forest areas. As evidenced by Mensah *et al.* (2015), miners clear large forest areas for gold ore exploration and extraction. While these actions have socio-economic effects, there is a spill-over effect because farmers and inhabitants are forced to clear other forest areas for new farmlands (Schueler *et al.*, 2011) and build houses. These actions consequently lead to the displacement of animals in their natural habitats and environmental degradation.

Between 2016 and 2024, mining areas increased by 10.640 km² (7.251%) and tailings dams and flooded areas by 33.283

km² (22.681%), indicating a peak in mining activity. This has led to a significant reduction in both dense and less dense vegetation, with serious environmental impacts including deforestation, loss of vegetation, and increased pollution from mining waste. Although Marfo *et al.* (2024) stipulated that Obuasi Municipal is located within a good water quality index zone, however, in the event of rainfall, the chemicals can be remobilised and enter the natural waterways where they can have an impact on aquatic ecosystems (Antwi-Agyei *et al.*, 2009). Faseyi *et al.* (2022) reported that continuous gold mining in the Pra and Ankobra estuaries has led to contamination of both water bodies with traces of cadmium, lead, mercury, and arsenic. These can cause growth retardation (Nyanza *et al.*, 2014), diarrhea (Emmanuel & Dzigbodi, 2018), tissue damage (Aitio *et al.*, 2022), anemia (Weinhouse *et al.*, 2017), and neurodegenerative diseases in humans (Lezak *et al.*, 2023) as well as oxidative stress in plants (Ngole-Jeme & Fantke, 2017). Considering the whole period from 1990 to 2024, mining areas increased by 27.655 km² (18.846%) and dam and flooded pits by 46.554 km² (31.724%), leading to long-term environmental degradation. In addition, the total area of dense vegetation, less dense vegetation, and built-up and bare land decreased, reflecting widespread landscape transformation and environmental impacts.

Predicting future LULC Changes due to Mining Activities

During the period from 2024 to 2032 (Table 4), a predictive analysis of LULC changes in the Obuasi municipality was conducted. The findings indicate a significant projected increase in mining areas from 27.655 km² to 52.179 km², representing a rise of 24.524 km² (16.712%). This escalation suggests an expansion in both legal and illegal mining operations, highlighting ongoing unauthorised mining activities. The unregulated expansion of illegal mining poses substantial risks to sustainable land management and environmental health in the region. Concurrently, the area for tailing dams and flooded areas is anticipated to decrease drastically from 46.554 km² to 19.141 km², reflecting a reduction of 27.412 km² (-18.680%). This decline may be indicative of the abandonment of tailing dams due to illegal mining activities, leaving polluted and hazardous sites without proper remediation. Alternatively, it may signal a shift in mining practices due to stricter regulations or enforcement against illegal mining. However, without effective management, these areas may continue to pose environmental hazards.

The forecast also presents a projected decrease in dense vegetation from 26.921 km² in 2024 to 18.179 km² in 2032, indicating a reduction of 8.742 km² (-5.957%). This ongoing loss of dense vegetation underscores the severe impact of illegal mining on forested areas, emphasising the need for robust measures to protect and restore forested areas. Additionally, less dense vegetation is anticipated to increase from 24.081 km² to 31.717 km², reflecting a rise of 7.636 km² (5.204%). This shift might indicate a transition from dense forests to less dense, degraded vegetation due to mining activities. This suggests the gradual degradation of the natural environment and the necessity for interventions to promote reforestation and sustainable land use practices. Built-up and bare land is projected to increase from 21.535 km² to 25.529 km², indicating an expansion of settlements and bare land, likely driven by the influx of populations associated with mining activities. This growth can exacerbate environmental degradation and strain local infrastructure and resources.

Limitation of Study

There are several limitations to using Landsat imagery to assess mining activities and changes in LULC. The 30-meter spatial resolution may not effectively capture smaller-scale mining activities and associated LULC changes, particularly for detecting small-scale illegal mining activities and minor environmental changes. In addition, Landsat imagery cannot detect underground mining activities, which limits a comprehensive assessment of the extent and intensity of all mining activities. Another challenge is the persistent cloud cover, especially in tropical regions such as Obuasi. Heavy cloud cover during the rainy season obscures the land surface, making it difficult to use available imagery effectively. Even partial cloud cover can significantly reduce image quality and obscure ground features, leading to errors in analysis, particularly in detecting small-scale changes in LULC. In the predictive model, the model did not factor in any external influence, such as policy changes or unforeseen environmental events, which may influence future LULC changes. This study did not include primary data on environmental issues such as pollution, health effects or biodiversity loss. The discussion of environmental impacts was based on existing literature rather than direct measurements or surveys. It also assumed that factors influencing LULC changes remain constant, which may introduce uncertainty. Future research should include field assessments and socio-economic data for a thorough analysis of the environmental and community impacts of mining.

CONCLUSIONS

In this paper, geospatial techniques were used to assess and quantify the impact of mining activities on LULC changes in the Obuasi municipality. The study examined LULC changes from 1990 to 2024 using Landsat imagery employing an RF classifier. The study highlights the significant environmental impacts of mining in the Obuasi Municipality. It emphasises the need for effective land management strategies and geospatial techniques to monitor and mitigate these impacts. The findings are critical for sustainable development policies and ensuring long-term ecological health. Identification of affected areas can assist in reforestation and land reclamation projects. The 2032 LULC model highlights significant LULC changes in the Obuasi Municipality due to mining activities, particularly illegal mining. The significant increase in mining areas and the corresponding decrease in dense vegetation and tailings dams indicate projected environmental degradation and the challenges of managing illegal mining. The predicted changes highlight the need for comprehensive strategies to address illegal mining. Therefore, the Environmental Protection Agency (EPA-Ghana), the Ghana Forestry Commission and the Ashanti Regional Coordination Council (ARCC) must enforce regulations more strictly, implement sustainable land management practices, and initiate restoration initiatives to mitigate adverse environmental impacts and promote ecological resilience in the municipality.

Data availability statement

Data will be made available on request.

Ethical statement

The authors declare that all ethical practices have been followed concerning the development, writing and publication of the work reported in this paper.

Declaration of interests

The authors declare that they have no known competing financial interests or personal relationships that could have appeared to influence the work reported in this paper.

Declaration of Competing Interest

The authors declare that they have no conflict of interest.

REFERENCES

Ababio, E., & Mensah, O.-. (2011). Gold mining and the socio-economic development of Obuasi in Adanse. *African Journal of History and Culture*, *3*(4), 54–64.

Adão, T., Hruška, J., Pádua, L., Bessa, J., Peres, E., Morais, R., & Sousa, J. J. (2017). Hyperspectral imaging: A review on UAV-based sensors, data processing and applications for agriculture and forestry. *Remote Sensing*, *9*(11), 1110. https://doi.org/10.3390/rs9111110

Adu-Baffour, F., Daum, T., & Birner, R. (2021). Governance challenges of small-scale gold mining in Ghana: Insights from a process net-map study. *Land Use Policy*, *102*(December 2020), 105271. https://doi.org/10.1016/j.landusepol.2020.105271

Adu-Poku, I., Drummond, J., & Li, Z. (2012). Land-cover change monitoring in Obuasi, Ghana: an integration of earth observation, geoinformation systems and stochastic modelling. *… of Earth Science and Engineering*, *2*(5), 1–14.

Aitio, A., Monica Nordberg, & Santonen, T. (2022). Chapter 14 - Gold and Gold mining. In G. F. Nordberg & M. Costa (Eds.), *Handbook on the Toxicology of Metals (Fifth Edition)* (Fifth Edition, pp. 317–351). Academic Press. https://doi.org/https://doi.org/10.1016/B978-0-12-822946-0.00013-1

Amankwah, A. A., Quaye-Ballard, J. A., Koomson, B., Amankwah, R. K., Awotwi, A., Kankam, B. O., Opuni-Frimpong, N. Y., Baah, D. S., & Adu-Bredu, S. (2021). Deforestation in forest-savannah transition zone of Ghana: Boabeng-Fiema monkey sanctuary. *Global Ecology and Conservation*, *25*, e01440. https://doi.org/10.1016/j.gecco.2020.e01440

Amoako-Attah, B. (2024). Analyzing Spatio-Temporal Trend of the Vegetative Cover of the Adansi South Cluster of Forest Reserves in Ghana. *International Journal of Multidisciplinary Studies and Innovative Research*, *12*(1), 1741–1751. https://doi.org/10.53075/Ijmsirq/0984568677264

Anarfi, K., Hill, R. A., & Shiel, C. (2020). Highlighting the sustainability implications of urbanisation: A comparative analysis of two urban areas in Ghana. *Land*, *9*(9), 1–24. https://doi.org/10.3390/LAND9090300

Anderson, C. (2007). USGS Anderson Land. *Estuaries*, *1976*, 1–10.

Anglogold Ashanti. (2021). *Obuasi, Ghana - AngloGold Ashanti*. https://www.anglogoldashanti.com/portfolio/africa/obuasi/

Antwi-Agyei, P., Hogarh, J. N., & Foli, G. (2009). Trace elements contamination of soils around gold mine tailings dams at Obuasi , Ghana. *African Journal of Environmental Science and Technology*, *3*(11), 353–359.

Ashiagbor, G., Amoako, C., Asabere, S. B., & Quaye-Ballard, J. A. (2019). Landscape Transformations in Rapidly Developing Peri-urban Areas of Accra, Ghana: Results of 30 years. *GeoScape*, *11*(1), 172–182. https://doi.org/10.1515/geo-2019-0014

Awotwi, A., Anornu, G. K., Quaye-Ballard, J. A., & Annor, T. (2018). Monitoring land use and land cover changes due to extensive gold mining, urban expansion, and agriculture in the Pra River Basin of Ghana, 1986–2025. *Land Degradation and Development*, *29*(10), 3331–3343. https://doi.org/10.1002/ldr.3093

Basommi, L. P., Guan, Q. ;, Cheng, D. ;, & Singh, S. K. (2016). Dynamics of land use change in a mining area : a case study of Nadowli District , Ghana. *J. Mt. Sci.*, *13*(4), 633–634.

Basommi, P. L., Guan, Q., & Cheng, D. (2015). Exploring Land use and Land cover change in the mining areas of Wa East District, Ghana using Satellite Imagery. *Open Geosciences*, *7*(1), 618–626. https://doi.org/10.1515/geo-2015-0058

Brovelli, M. A., Sun, Y., & Yordanov, V. (2020). Monitoring forest change in the amazon using multi-temporal remote sensing data and machine learning classification on Google Earth Engine. *ISPRS International Journal of Geo-Information*, *9*(10), 1–21. https://doi.org/10.3390/ijgi9100580

Brundtland, G. H. (1985). World commission on environment and development. *Environmental Policy and Law*, *14*(1), 26–30.

Cheruto, M. C., Kauti, M. K., Kisangau, P. D., & Kariuki, P. (2016). Assessment of Land Use and Land Cover Change Using GIS and Remote Sensing Techniques: A Case Study of Makueni County, Kenya. *Journal of Remote Sensing & GIS*, *05*(04). https://doi.org/10.4172/2469-4134.1000175

Cobbinah, P. B., Erdiaw-Kwasie, M. O., & Amoateng, P. (2015). Africa's urbanisation: Implications for sustainable development. *Cities*, *47*, 62–72. https://doi.org/10.1016/j.cities.2015.03.013

El Baroudy, A. A. (2011). Monitoring land degradation using remote sensing and gis techniques in an area of the middle Nile Delta, Egypt. *Catena*, *87*(2), 201–208. https://doi.org/10.1016/j.catena.2011.05.023

Ellimah, R. (2022). Return of Anglogold Ashanti: Will Obuasi Rise Again? *New Agenda: South African Journal of Social and Economic Policy*, *2022*(83), 53–55. https://doi.org/10.10520/ejc-nagenda_v2022_n83_a11

Emmanuel, J., & Dzigbodi. (2018). Environmental and Health Impacts of Mining in Ghana. In *Journal of Health & Pollution* (Vol. 8, Issue 17).

Faseyi, C. A., Miyittah, M. K., Sowunmi, A. A., & Yafetto, L. (2022). Water quality and health risk assessments of illegal gold mining-impacted estuaries in Ghana. *Marine Pollution Bulletin*, *185*(PA), 114277. https://doi.org/10.1016/j.marpolbul.2022.114277

Gandharum, L., Hartono, D. M., Karsidi, A., & Ahmad, M. (2022). Monitoring Urban Expansion and Loss of Agriculture on the North Coast of West Java Province, Indonesia, Using Google Earth Engine and Intensity Analysis. *Scientific World Journal*, *2022*(Sdg 2). https://doi.org/10.1155/2022/3123788

Gbedzi, D. D., Ofosu, E. A., Mortey, E. M., Obiri-Yeboah, A., Nyantakyi, E. K., Siabi, E. K., Abdallah, F., Domfeh, M. K., & Amankwah-Minkah, A. (2022). Impact of mining on land use land cover change and water quality in the Asutifi North District of Ghana, West Africa. *Environmental Challenges*, *6*(August 2021). https://doi.org/10.1016/j.envc.2022.100441

Ghana Statistical Service. (2021). *Ghana 2021 Population And Housing Census, General Report*. *3A*, 128.

Gondwe, J. F., Lin, S., & Munthali, R. M. (2021). Analysis of Land Use and Land Cover Changes in Urban Areas Using Remote Sensing: Case of Blantyre City. *Discrete Dynamics in Nature and Society*, *2021*. https://doi.org/10.1155/2021/8011565

GR. (2022). *Ashanti Region - GhanaRegions.com*. https://ghanaregions.com/ashanti-region/

Koranteng, A., & Zawila-Niedzwiecki, T. (2015). Modelling forest loss and other land use change dynamics in Ashanti Region of Ghana. *Folia Forestalia Polonica, Series A*, *57*(2), 96–111. https://doi.org/10.1515/ffp-2015-0010

Kossoff, D., Dubbin, W. E., Alfredsson, M., Edwards, S. J., Macklin, M. G., & Hudson-Edwards, K. A. (2014). Mine tailings dams: Characteristics, failure, environmental impacts, and remediation. *Applied Geochemistry*, *51*, 229–245. https://doi.org/10.1016/j.apgeochem.2014.09.010

Kwaning, E., & Atteh, E. (2022). Review on Effects of Mining in Ghana: The Case of Obuasi Municipality. *Asian Research Journal of Arts & Social Sciences*, *18*(4), 50–57. https://doi.org/10.9734/arjass/2022/v18i4402

Lezak, S., Wilson, C., Ansar, A., & Bazilian, M. (2023). The case against gold mining. *Environmental Research Letters*, *18*(1). https://doi.org/10.1088/1748-9326/ac9f26

Loveland, T. R., & Dwyer, J. L. (2012). Landsat: Building a strong future. *Remote Sensing of Environment*, *122*, 22–29. https://doi.org/10.1016/j.rse.2011.09.022

Loveland, T. R., & Irons, J. R. (2016). Landsat 8: The plans, the reality, and the legacy. *Remote Sensing of Environment*, *185*, 1–6. https://doi.org/10.1016/j.rse.2016.07.033

Mahboob, M. A., Atif, I., & Iqbal, J. (2015). Remote Sensing and GIS Applications for Assessment of Urban Sprawl in Karachi, Pakistan. *Science, Technology and Development*, *34*(3), 179–188. https://doi.org/10.3923/std.2015.179.188

Marfo, J. N., Quaye-Ballard, J. A., Kwakye, S. O., Obeng, K., Arko-Adjei, A., Quaye-Ballard, N. L., & Quao, R. N. A. (2024). Groundwater quality and potential analysis using geospatial techniques: The case of Ashanti Region in Ghana. *Heliyon*, *10*(6), e27545. https://doi.org/10.1016/j.heliyon.2024.e27545

Matarira, D., Mutanga, O., & Naidu, M. (2022). Google Earth Engine for Informal Settlement Mapping: A Random Forest Classification Using Spectral and Textural Information. *Remote Sensing*, *14*(20). https://doi.org/10.3390/rs14205130

Mensah, A. K., Mahiri, I. O., Owusu, O., Mireku, O. D., Wireko, I., & Kissi, E. A. (2015). Environmental Impacts of Mining: A Study of Mining Communities in Ghana. *Applied Ecology and Environmental Sciences*, *3*(3), 81–94. https://doi.org/10.12691/aees-3-3-3

Mensah, E., Wapaburda, S., & Hammond, F. (2017). A hybrid image classification approach to monitoring LULC changes in the mining district of Prestea-huni Valley, Ghana. *Journal of Environment and Earth Science*, *7*(3), 10.

Mohamed, E. S., Belal, A., & Saleh, A. (2013). Assessment of land degradation east of the Nile Delta, Egypt using remote sensing and GIS techniques. *Arabian Journal of Geosciences*, *6*(8), 2843–2853. https://doi.org/10.1007/s12517-012-0553-2

Nelson, S. A. C., Khorram, S., & Dorgan, S. (2020). Image Processing and Data Analysis with ERDAS IMAGINE. In *Photogrammetric Engineering & Remote Sensing* (Vol. 86, Issue 10). https://doi.org/10.14358/pers.86.10.597

Ngole-Jeme, V. M., & Fantke, P. (2017). Ecological and human health risks associated with abandoned gold mine tailings contaminated soil. *PLoS ONE*, *12*(2). https://doi.org/10.1371/journal.pone.0172517

Ngom, N. M., Baratoux, D., Bolay, M., Dessertine, A., Abass Saley, A., Baratoux, L., Mbaye, M., Faye, G., Yao, A. K., & Kouamé, K. J. (2023). Artisanal Exploitation of Mineral Resources: Remote Sensing Observations of Environmental Consequences, Social and Ethical Aspects. *Surveys in Geophysics*, *44*(1), 225–247. https://doi.org/10.1007/s10712-022-09740-1

Nunoo, S., Manu, J., Owusu-Akyaw, F. K. B., & Nyame, F. K. (2022). Impact of artisanal small-scale (gold and diamond) mining activities on the Offin, Oda and Pra rivers in Southern Ghana, West Africa: A scientific response to public concern. *Heliyon*, *8*(12), e12323. https://doi.org/10.1016/j.heliyon.2022.e12323

Nyame, F. K., & Blocher, J. (2010). Influence of land tenure practices on artisanal mining activity in Ghana. *Resources Policy*, *35*(1), 47–53. https://doi.org/10.1016/j.resourpol.2009.11.001

Nyanza, E. C., Joseph, M., Premji, S. S., Thomas, D. S. K., & Mannion, C. (2014). Geophagy practices and the content of chemical elements in the soil eaten by pregnant women in artisanal and small scale gold mining communities in Tanzania. *BMC Pregnancy and Childbirth*, *14*(1). https://doi.org/10.1186/1471-2393-14-144

Opoku;, M. P., Mensah;, J. K., Griffith, B. A. A., & 9, S. N. N. (2015). Impact of mining in Obuasi Municipality in Ashanti region of Ghana : An assessment of human rights concerns in mining communities. *Scholars Journal of Arts , Humanities and Social Sciences*, *3*(9A), 1407–1415.

Pachón, I., Ramírez, S., Fonseca, D., Lozano-Rivera, P., Ariza, C., Mancipe, M. P., Villamizar, M., Castro, H., Cabrera, E., & Becerra, M. T. (2018). Random forest data cube based algorithm for land cover classification: A colombian case. *International Geoscience and Remote Sensing Symposium (IGARSS)*, *2018-July*, 8651–8654. https://doi.org/10.1109/IGARSS.2018.8518480

Pereira, V., Tuffour, J., Patnaik, S., Temouri, Y., Malik, A., & Singh, S. K. (2021). The quest for CSR: Mapping responsible and irresponsible practices in an intra-organizational context in Ghana's gold mining industry. *Journal of Business Research*, *135*(June), 268–281. https://doi.org/10.1016/j.jbusres.2021.06.024

Ros-Tonen, M. A. F., Aggrey, J. J., Somuah, D. P., & Derkyi, M. (2021). Human insecurities in gold mining: A systematic review of evidence from Ghana. *Extractive Industries and Society*, *8*(4), 1–16. https://doi.org/10.1016/j.exis.2021.100951

Sarma, K., & Kushwaha, S. P. S. (2005). coal mining impact on land use/land cover in jaintia hills district of Meghalaya, India using remote sensing and GIS technique. *Conference Proceeding of National Conference on Geospatial Technologies, Geomatrix*, *9*(2005), 28–43.

Schueler, V., Kuemmerle, T., & Schröder, H. (2011). Impacts of surface gold mining on land use systems in Western Ghana. *Ambio*, *40*(5), 528–539. https://doi.org/10.1007/s13280-011-0141-9

Singh, P., Kikon, N., & Verma, P. (2017). Impact of land use change and urbanization on urban heat island in Lucknow city, Central India. A remote sensing based estimate. *Sustainable Cities and Society*, *32*, 100–114. https://doi.org/10.1016/j.scs.2017.02.018

Toure, S. I., Stow, D. A., Clarke, K., & Weeks, J. (2020). Patterns of land cover and land use change within the two major metropolitan areas of Ghana. *Geocarto International*, *35*(2), 209–223. https://doi.org/10.1080/10106049.2018.1516244

Weinhouse, C., Ortiz, E. J., Berky, A. J., Bullins, P., Hare-Grogg, J., Rogers, L., Morales, A. M., Hsu-Kim, H., & Pan, W. K. (2017). Hair mercury level is associated with anemia and micronutrient status in children living near artisanal and small-scale gold mining in the Peruvian Amazon. *American Journal of Tropical Medicine and Hygiene*, *97*(6), 1886–1897. https://doi.org/10.4269/ajtmh.17-0269

Yankson, P. W. K., & Gough, K. V. (2019). Gold in Ghana: The effects of changes in large-scale mining on artisanal and small-scale mining (ASM). *Extractive Industries and Society*, *6*(1), 120–128. https://doi.org/10.1016/j.exis.2018.09.009

Yiridomoh, G. Y. (2021). "Illegal" Gold Mining Operations in Ghana: Implication for Climate-Smart Agriculture in Northwestern Ghana. *Frontiers in Sustainable Food Systems*, *5*(December), 1–12. https://doi.org/10.3389/fsufs.2021.745317

Yordanov, V., & Brovelli, M. A. (2021). Deforestation mapping using sentinel-1 and object-based random forest classification on google earth engine. *International Archives of the Photogrammetry, Remote Sensing and Spatial Information Sciences - ISPRS Archives*, *43*(B3-2021), 865–872. https://doi.org/10.5194/isprs-archives-XLIII-B3-2021-865-2021

Zareie, S., Khosravi, H., Nasiri, A., & Dastorani, M. (2016). Using Landsat Thematic Mapper (TM) sensor to detect change in land surface temperature in relation to land use change in Yazd, Iran. *Solid Earth*, *7*(6), 1551–1564. https://doi.org/10.5194/se-7-1551-2016

Zhou, L., Dang, X., Sun, Q., & Wang, S. (2020). Multi-scenario simulation of urban land change in Shanghai by random forest and CA-Markov model. *Sustainable Cities and Society*, *55*(January), 102045. https://doi.org/10.1016/j.scs.2020.102045